COMMUNICATION

Tuning Crystalline Solid-State Order and Charge Transport via Building-Block Modification of Oligothiophenes

By *Colin Reese, Mark E. Roberts, Sean R. Parkin,* and *Zhenan Bao**

Organic electronic materials have been the focus of intense research for more than twenty years. In addition to their oft-cited potential advantages of low-cost, compatibility with plastic substrates, and ease of processing, much of their appeal lies in the promise of functionality and performance by design.[1,2] Ideally, electronic materials for applications ranging from flexible circuits and displays to radio frequency identification (RFID) tags, light-emitting diodes (LEDs), and chemical sensors will be synthesized on demand from a toolbox of organic components. While the field has yet to realize such lofty goals, the development of a library of organic electronic materials and new experimental techniques have offered structure–property relationships that will serve as the foundation for the development of the *a priori* prediction of optoelectronic properties.

The highest performance organic semiconductors have the common feature of a delocalized, aromatic, electronically active core. Fused acenes, thiophenes, and oligothiophenes are prototypical systems that are comprised of only this component, and have demonstrated benchmark performance.[3] Because the molecular subunits are relatively non-polar, however, intermolecular interactions are rather weak. The electronic homogeneity of the units results in crystal structures bound loosely by van der Waals forces that are only weakly favored thermodynamically. Experimentally, this is observed in the form of polymorphism and crystal disorder, as has been observed for linear acenes,[4,5] as well as a plethora of oligothiophenes,[4] even for some cases of substitutions designed to impart order (see reference [6] within Azumi et al.[7]). The result of this phenomenon is a solid-state order and organization that is both difficult to predict and control.

One approach to predictably imparting order involves functionalizing an aromatic core with bulky pendant groups,[5,6] which strongly direct supramolecular organization through steric repulsion. While this provides for a wide variety of crystal packing motifs and often improves performance through increased order, it often has the side effect of spacing molecules more disparately or at disadvantageous orientations, which may actually impair transport. In particular, while functionalization at the center of the electronically active core very uniquely specifies a packing motif based on the relative sizes of bulky groups and aromatic moieties,[8,9] it often has the effect of limiting longitudinal alignment of the cores.

Here, we study the family of α-substituted oligothiophene derivatives shown in Figure 1 (see Supporting information, SI, for synthesis details) in order to determine the effects of terminal substituent density on the packing of the electronically active core units. The molecules consist of an aromatic oligothiophene core, functionalized at the terminal positions with trimethylsilane (TMS) groups. In addition to imparting solubility, the substituent TMS groups yield layer-by-layer ordering of the aromatic cores. By isolating the functionalization to the terminal positions, the TMS groups are isolated to between the bc-planes that dominate charge transport. Furthermore, this motif allows us to study specifically the steric effects of the TMS groups on the in-plane packing of the aromatic core. Our previous thin-film structure studies showed that end substitution on the aromatic molecule with[10] less bulky linear alkyl chains did not change the molecular packing motif.

To examine the effect of the terminal TMS substitutions on the molecular packing, single crystals were grown using the Physical Vapor Transport technique[11] and characterized by X-Ray diffraction (see SI for details). All of the compounds in Figure 1 formed thin, nearly two-dimensional platelet crystals, ideal for single crystal transistor device fabrication.[12] The TMS-substituted compounds were especially stable, leaving behind no starting material, even if melted prior to crystal growth. The structures of the single crystals of quaterthiophene (4T) and TMS-substituted

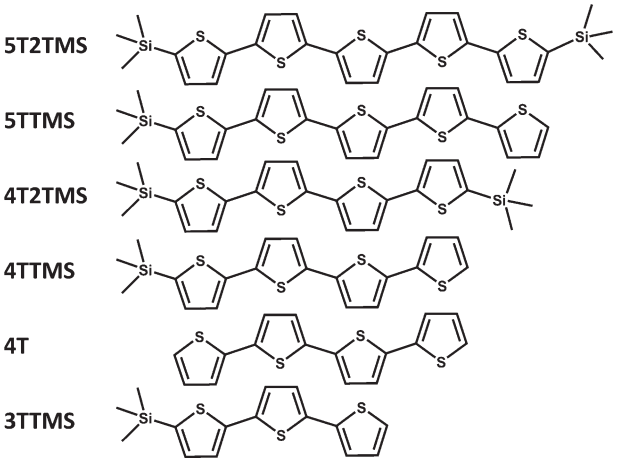

Figure 1. Chemical structures of the oligothiophene and derivatives studied here.

[*] Prof. Z. Bao, Dr. C. Reese, Dr. M. E. Roberts
Department of Chemical Engineering, Stanford University
381 North-South Mall, Stanford, CA 94305 (USA)
E-mail: zbao@stanford.edu
Dr. S. R. Parkin
Department of Chemistry, University of Kentucky
Lexington, KY 40506-0055 (USA)

DOI: 10.1002/adma.200900836

derivatives are shown in Figure 2. All adopt a standard layer-by-layer herringbone motif, with the tilt angle (δ, cf. Fig. 2) of the molecules within the bc-plane determined by the terminal substitution. For the monosubstituted 4TTMS, the alternating TMS groups between layers allow the oligothiophene cores to arrange nearly vertically ($\delta = 26^\circ$), so as to arrange the bulky groups in nearly equidistant, space-filling fashion. In contrast, the disubstituted 4T2TMS is unable to accommodate twice the density of TMS between layers in an upright position, and the molecule must tilt severely ($\delta = 51^\circ$) to stagger the units. The unsubstituted 4T is arranged to best suit the weak intermolecular interactions, and tilts at an angle ($\delta = 34^\circ$) intermediate that of 4TTMS and 4T2TMS. In addition to the near-vertical arrangement of the quaterthiophene cores, mono-TMS substitution also results in increased crystal symmetry. While 4T and 4T2TMS exhibit monoclinic symmetry, 4TTMS is orthorhombic. Furthermore, the unit axes' lengths of the 4TTMS crystal are within 19% of each other, compared with a 45% and 63% 4T and 4T2TMS, respectively. This isotropy has implications for in-plane charge transport.[13] While the other oligothiophenes' (3T, 5T) and their derivatives' crystal structures were not determined, the steric effects that determine their arrangement remain the same. Oligothiophenes and other aromatics terminated with alkyl[14] or other[15] groups, for example, exhibit the same packing motifs regardless of core size. Accordingly, it is reasonable to assume that they demonstrate the same trends for 3T and 5T analogues.

In order to determine how the microscopic arrangement of the oligothiophene derivatives is manifested in their macroscopic electronic properties, vapor-grown crystals were used to construct elastomeric single-crystal field-effect transistors (SCFETs), as described previously.[16,17] The especially thin crystals formed by TMS-substituted derivatives were especially amenable to device fabrication, resulting in excellent device yield, crystal contact, and electrical characteristics. Unsubstituted 4T also produced two-dimensional crystals, but varying in size, quality and thickness. The thinner crystals were cellophane-like in appearance and less mechanically rigid, while all substituted crystals were uniform, with glass-like appearance. The devices were tested in air immediately after growth and fabrication. While TMS-substituted derivatives showed stability over days, the field-effect mobility of 4T degraded upon exposure to air over the course of less than an hour under intermittent bias. This contrast is unsurprising: degradation of unpassivated organics such as fused acenes[18] and polythiophenes[19] is well-documented in literature. On the other hand, hydrophobic alkyl groups or other nonpolar moieties have been shown to increase resistance to penetration by agents that assist degradation, such as water and oxygen.[20]

The field-effect mobilities, as extracted in the saturation regime using the standard methods,[21] are shown in Figure 3. The most obvious trend is within the quaterthiophene series, for which performance increases from 0.03 to 0.13 to 0.23 $cm^2\ V^{-1}\ s^{-1}$ from 4T2TMS to 4TTMS to 4T. A weaker trend is also observed with an increase in oligothiophene length in the monosubstituted nTTMS series. Without 3T2TMS or sufficient mobility resolution for the nT2TMS series (a trend of the same magnitude or percentage as the nTTMS series would be within experimental error), it is difficult to determine whether the same trend holds. What is clear, however, is that intermolecular interactions represent the most critical difference, while conjugation length yields very little difference for similar functionality. This is contrary to popular heuristics for the development of high-performance semiconductors, which generally state sufficient conjugation as a primary requisite for acceptable performance—in order for the transport energy levels to align with the contact workfunction.[22,23] In particular, for a terthiophene (3T) derivative to show a mobility in the same order of magnitude as the 5T analogue is unusual. As calculation and experiment have shown recently, however, transport in organics is intrinsically extremely sensitive to molecular proximity and orientation.[5,24]

In order to more accurately correlate the observed performance trends to the crystal structure, electronic structure calculations were carried out on the coordinates of 4T, 4TTMS, and 4T2TMS, as determined by X-Ray diffraction and shown in Figure 2. Single-point dimer calculations were employed to determine the intermolecular overlap of molecular orbitals, as manifested in the transfer integral (t).[22] These calculations, carried out at the B3LYP/6-311G* level, are shown in Table 1. As previously reported,[25] nearest-neighbor polarization is a component of dimer-calculated transfer integrals, and

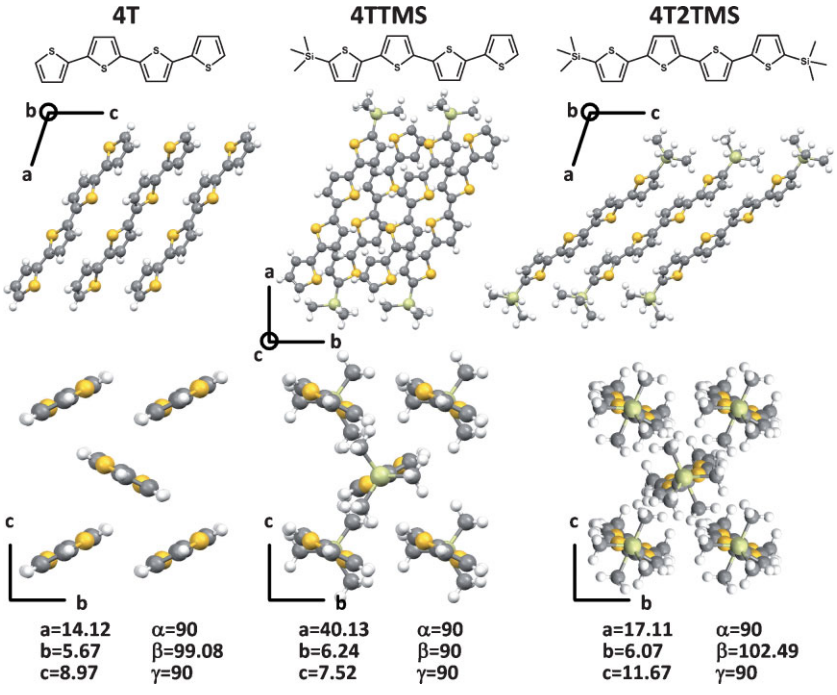

Figure 2. Chemical and crystal structures and lattice parameters of a subset of the molecules studied: unsubstituted (4T), mono-TMS (4TTMS) and di-TMS quaterthiophene (4T2TMS). Terminal substitution determines the in-plane tilt (δ) of the oligothiophene cores, with 4T2TMS(51°) > 4T(34°) > 4TTMS(26°).

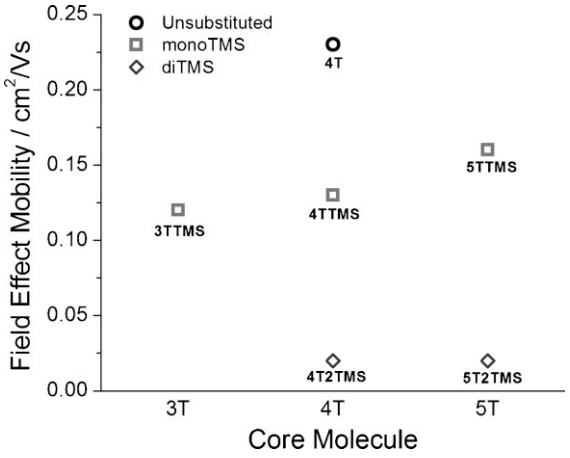

Figure 3. Field-effect mobilities of single crystals of the oligothiophene derivatives shown, characterized in the saturation regime using elastomeric single-crystal field-effect transistors.

may convolute the direct interpretation of calculations based on the dimer technique, particularly when comparing differing functionalities and/or edge/face versus stacked interactions. For this analysis, however, we reserve our comparisons to both identical functionality and similar (edge/face) interactions, the only non-negligible highest-occupied molecular orbital (HOMO) overlap between quaterthiophene cores (for the transport of holes probed here, HOMO transfer integrals are those of interest).

Despite the vertical orientation of the thiophene core imparted by the single TMS unit, the 4T series is ranked 4T2TMS < 4TTMS < 4T in terms of both $\langle 1/2, 1/2\rangle$, and $\langle 1/2, -1/2\rangle$ edge/face interaction strength along the unit cell diagonals, with 4TTMS and 4T besting the transfer integral of 4T2TMS by 31 and 23 percent, respectively. This trend is clear, as is the matching trend in measured field-effect mobility. Comparing the calculated interaction strengths to the crystal structures, it seems counter-intuitive that 4T should perform better than 4TTMS, as 4T is further slipped along its long axis in relation to its nearest neighbor and hence has less thiophene overlap. As shown amply by experiment and calculation,[5,24] however, the efficiency of orbital overlap is extremely sensitive to the nodal structure of the relevant frontier molecular orbitals. In this case, the increased edge/face overlap of the upright 4TTMS molecules is compensated for by the efficiency of the 4T diagonal overlap. The tilted structure of 4T2TMS, on the other hand, results in an offset of the quaterthiophene cores by more than a full thiophene unit, and a corresponding diminished transfer integral.

Table 1. HOMO and LUMO transfer integrals in meV for 4T, 4T-TMS, and 4T-2TMS, calculated at the B3LYP-6-311G* level.

	4T		4T-TMS		4T-2TMS	
	LUMO	HOMO	LUMO	HOMO	LUMO	HOMO
$\langle 1,0\rangle$[a]	105.3	1.4	90.6	5.4	61.9	4.2
$\langle 0,1\rangle$	0.8	0.0	7.2	3.4	0.7	0.3
$\langle 1/2,1/2\rangle$	152.1	156.5	154.8	146.9	122.0	119.1
$\langle 1/2,-1/2\rangle$	151.7	156.5	143.3	136.1	121.8	119.1

[a] Expressed in terms of the crystal axis vectors $\langle b,c\rangle$.

In conclusion, we have shown that the orientation and proximity of organic semiconductor molecules in the solid-state may be tuned using a terminal building-block-type modification, resulting in substantial quantitative and qualitative differences in their electronic properties. Specifically, the addition of a terminal TMS group results in crystal packing that directly reflects the steric considerations of their interlayer confinement. This is indirectly manifested in the tilt and offset of the oligothiophene cores responsible for charge transport within the *bc*-plane: mono and di-substituted quaterthiophenes showed less and more tilt/offset, respectively, than their unsubstituted counterpart. These differences were apparent in their intermolecular electronic interactions, as measured macroscopically via electrical characterization and calculated using quantum chemical calculations and the resolved crystal structures. The predicted and measured trend was coincident, with 4T > 4TTMS > 4T2TMS in terms of charge transport efficiency. While the data are insufficient to apply the general conclusion to the oligomers 3T and 5T, electrical comparison of the monoTMS series, in particular between 5TTMS and 5T2TMS, suggests that the trend holds. Furthermore, structural comparisons of analogues varying only in core length have demonstrated identical motifs.[14,15] This work demonstrates that substantial modification of the intermolecular interactions may be effected by the proper tuning of terminal groups, subtly tuning longitudinal offset of the aromatic cores. Furthermore, the correlation of these results with direct calculation suggests that solid-state tuning via steric interactions with predictable results is indeed possible.

Experimental

Material Synthesis: [2,2′;5′,2″;5″,2‴]Quaterthiophene (**4T**) [26], 5,5‴-bis-trimethylsilanyl-[2,2′;5′,2″;5″,2‴]quaterthiophene (**4T2TMS**) [27], and trimethyl-[2,2′;5′,2″;5″,2‴]quaterthiophen-5-yl-silane (**4TTMS**) [20] and trimethyl-[2,2′;5′,2″]terthiophen-5-yl-silane (**3TTMS**) [28] were synthesized as previously reported.

5,5⁗-Bis-trimethylsilanyl-[2,2′;5′,2″;5″,2‴;5‴,2⁗]quinquethiophene (**5T2TMS**). To a nitrogen-flushed, two-neck flask was added 2,5-dibromothiophene (1.00 g, 4.13 mmol) and trimethyl-(5′-tributylstannanyl-[2,2′]bithiophenyl-5-yl)-silane [20] (5.23 g, 9.92 mmol) in 20 mL of anhydrous *N*,*N*-dimethylformamide. The solution was degassed by using freeze–pump–thaw until no gas evolved. Tetrakis(triphenylphosphine)palladium(0) (240 mg, 0.21 mmol) was added, and the reaction mixture was heated to 90 °C for 24 h. After cooling to room temperature, the mixture was poured into methanol and the precipitate was filtered. The crude product was flashed through silica gel in chloroform (1.21 g, 53%). The product was further purified by temperature gradient sublimation at 10^{-6} Torr (1 Torr = 133.32 Pa) and collected at 160–170 °C yielding a bright orange crystals. ^{1}H NMR (400 MHz, $CDCl_3$, δ): 7.23 (d, J = 3.6 Hz, 2H; ArH), 7.14 (d, J = 3.6 Hz, 2H; ArH), 7.09 (dd, J = 8.0 Hz, J = 4.0 Hz, 4H, ArH); 7.07 (s, 2H; ArH), 0.34 (s, 18H, CH_3). MS (ESI/APCI, m/z): 556.0 [M^+ – H].

Trimethyl-[2,2′;5′,2″;5″,2‴;5‴,2⁗;5⁗,2⁗′]quinquethiophen-5-yl-silane (**5TTMS**). To a nitrogen-flushed, two-neck flask was added 2-bromothiophene (0.061 g, 0.371 mmol) and TMSn-4TTMS (0.175 g, 0.3095 mmol) in 10 mL of anhydrous *N*,*N*-dimethylformamide. The solution was degassed by using freeze–pump–thaw until no gas evolved. Tetrakis(triphenylphosphine)palladium(0) (16 mg, 0.014 mmol) was added, and the reaction mixture was heated to 85 °C for 16 h. After cooling to room temperature, the mixture was poured into methanol and the precipitate was filtered. The crude product was flashed through silica gel in methylene chloride (104.5 mg, 70%). The product was further purified by temperature gradient

sublimation at 10^{-6} Torr and collected at 165–170 °C yielding a bright orange powder. ^{1}H NMR (400 MHz, $CDCl_3$, δ): 7.23 (d, $J = 3.6$ Hz, 2H; ArH), 7.18 (d, $J = 3.2$ Hz, 1H; ArH), 7.14 (d, $J = 3.2$ Hz, 1H; ArH), 7.07–7.10 (m, 6H; Ar H), 7.03 (dd, $J = 5.2$ Hz, $J = 3.6$ Hz, 1H; ArH), 0.34 (s, 9H; CH_3). MS (ESI/APCI, m/z): 484.0 [$M^+ - H$].

Trimethyl-(5‴-trimethylstannanyl-[2,2′;5′,2″;5″,2‴]quaterthiophen-5-yl)-silane (TMSn-4TTMS). To a nitrogen-flushed flask was added 4TTMS (0.5 g, 1.24 mmol) in 65 mL of anhydrous tetrahydrofuran (THF). The solution was bubbled with nitrogen for 30 min and then cooled to −78 °C. 2.5 M *n*-BuLi (0.55 mL, 1.37 mmol) in hexanes was added dropwise over 30 min, and the mixture was stirred for 1 h and allowed to warm to 25 °C. The reaction mixture was then cooled to −78 °C, and then quenched with 1 M trimethyltin chloride (1.31 mL, 1.30 mmol) in THF. The mixture was allowed to warm to room temperature and stir for 4 h, then poured into 100 mL of ammonium chloride. The product was extracted with methylene chloride, washed with 50 mL of 5% NH_4Cl (× 3) and H_2O (× 3). The solution was dried over $MgSO_4$ and then the solvent was removed by evaporation at reduced pressure. The product was recrystallized in chloroform with a trace amount of methanol (0.13 g, 62%) yielding metallic green flakes. ^{1}H NMR ($CDCl_3$, 400 MHz, δ): 7.28 (d, $J = 3.2$ Hz, 1H; ArH), 7.22 (d, $J = 3.6$ Hz, 1H; ArH), 7.14 (d, $J = 3.6$ Hz, 1H; ArH), 7.09 (dd, $J = 8.0$ Hz, $J = 4.0$ Hz, 2H; ArH), 7.07 (s, 2H; ArH), 7.06 (d, $J = 3.2$ Hz, 1H; ArH), 0.39 (s, 9H; $SnCH_3$), 0.34 (s, 9H; $SiCH_3$).

Crystal Growth: Single crystals were grown by the physical vapor transport method [29] at atmospheric pressure in semiconductor-grade argon at approximately 80ccm; the details of this setup are described elsewhere [30]. All materials formed two-dimensional platelets, with TMS-substituted derivatives producing crystals relatively monodisperse in size and thickness, while 4T yielded crystals of varying quality. All were yellowish/clear, depending on crystal thickness.

Device Fabrication and Characterization: Transistors were fabricated as previously reported [16]. Devices had channel lengths of 10–100 μm, all with W/L of 10. Transistors were characterized using a Keithley 4200SCS and standard probe station setup in air. Devices were tested in both linear and saturation regimes and the device parameters were extracted using the standard calculation techniques [21]. Dielectric capacitance was measured using both the charge integration technique and by thickness. For additional details of characterization, see SI.

Crystal Analysis: X-ray data were collected on a Bruker-Nonius X8 Proteum CCD diffractometer using Cu Kα radiation. The structures were solved using SHELXS and refined using SHELXL from the SHELX-97 program package [31]. Molecular fragment editing was performed using the XP program of SHELXTL 5.0 [31]. All non-hydrogen atoms were refined with anisotropic displacement parameters. Hydrogen atoms were found in difference-Fourier maps and subsequently placed at calculated positions and refined using an appropriate riding model. The crystal used was an inversion twin with non-equal components (approximately 88:12). The relatively high *R*-value is largely a consequence of poor counting statistics caused by the thinness of the crystals.

Acknowledgements

C.R. acknowledges support from the AFCEA graduate fellowship. Work was performed in part at the Stanford Nanofabrication Facility of NNIN supported by the National Science Foundation under Grant ECS-9731293. M.E.R acknowledges partial support from NASA GSRP. Supporting Information is available online from Wiley InterScience or from the author.

Received: March 9, 2009
Revised: April 8, 2009
Published online: May 21, 2009

[1] C. Reese, M. Roberts, M.-M. Ling, Z. Bao, *Mater. Today* **2004**, *7*, 20.
[2] C. D. Dimitrakopoulos, P. R. L. Malenfant, *Adv. Mater.* **2002**, *14*, 99.
[3] a) *Organic Field-Effect Transistors*, Vol. *128*, CRC Press, Taylor and Francis, Boca Raton, FL **2007**. b) A. R. Murphy, J. M. J. Frechet, *Chem. Rev.* **2007**, *107*, 1066.
[4] E. Venuti, R. G. Della Valle, L. Farina, A. Brillante, M. Masino, A. Girlando, *Phys. Rev. B* **2004**, *70*, 104106.
[5] A. Troisi, G. Orlandi, *J. Phys. Chem. B* **2005**, *109*, 1849.
[6] a) L. Antolini, G. Horowitz, F. Kouki, F. Garnier, *Adv. Mater.* **1998**, *10*, 382. b) R. Azumi, E. Mena-Osteritz, R. Boese, J. Benet-Buchholz, P. Bauerle, *J. Mater. Chem.* **2006**, *16*, 728.
[7] H. Moon, R. Zeis, E. J. Borkent, C. Besnard, A. J. Lovinger, T. Siegrist, C. Kloc, Z. N. Bao, *J. Am. Chem. Soc.* **2004**, *126*, 15322.
[8] M. M. Payne, S. R. Parkin, J. E. Anthony, C. C. Kuo, T. N. Jackson, *J. Am. Chem. Soc.* **2005**, *127*, 4986.
[9] a) Z. N. Bao, A. J. Lovinger, *Chem. Mater.* **1999**, *11*, 2607. b) B. S. Ong, Y. L. Wu, P. Liu, *Proc. IEEE* **2005**, *93*, 1412.
[10] Q. Yuan, S. C. B. Mannsfeld, M. L. Tang, M. Roberts, M. F. Toney, D. M. DeLongchamp, Z. Bao, *Chem. Mater.* **2008**, *20*, 2763.
[11] R. A. Laudise, C. Kloc, P.G. Simpkins, T. Siegrist, *J. Cryst. Growth,* **1998**, *187*, 449.
[12] A. L. Briseno, R. J. Tseng, M. M. Ling, E. H. L. Falcao, Y. Yang, F. Wudl, Z. Bao, *Adv. Mater.* **2006**, *18*, 2320.
[13] C. Reese, M. Roberts, S. R. Parkin, Z. Bao, *App. Phys. Lett.* **2009**, *94*, DOI: 10.1063/1.3129162.
[14] a) C. D. Dimitrakopoulos, B. K. Furman, T. Graham, S. Hegde, S. Purushothaman, *Synth. Met.* **1998**, *92*, 47. b) M. Moret, M. Campione, A. Borghesi, L. Miozzo, A. Sassella, S. Trabattoni, B. Lotz, A. Thierry, *J. Mater. Chem.* **2005**, *15*, 2444.
[15] a) G. Barbarella, P. Ostoja, P. Maccagnani, O. Pudova, L. Antolini, D. Casarini, A. Bongini, *Chem. Mater.* **1998**, *10*, 3683. b) S. Hotta, M. Goto, R. Azumi, M. Inoue, M. Ichikawa, Y. Taniguchi, *Chem. Mater.* **2004**, *16*, 237.
[16] C. Reese, W.-J. Chung, M.-M. Ling, M. Roberts, Z. Bao, *Appl. Phys. Lett.* **2006**, *89*, 202108.
[17] a) C. Reese, Z. Bao, *Adv. Mater.* **2007**, *19*, 4535. b) C. Reese, Z. Bao, *Adv. Funct. Mater.* in press.
[18] C. Pannemann, T. Diekmann, U. Hilleringmann, *J. Mater. Res.* **2004**, *19*, 1999.
[19] M. L. Chabinyc, R. A. Street, J. E. Northrup, *Appl. Phys. Lett.* **2007**, *90*, 123508.
[20] M. E. Roberts, S. C. B. Mannsfeld, N. Queraltó, C. Reese, J. Locklin, W. Knoll, Z. Bao, *Proc. Natl. Acad. Sci. USA* **2008**, *105*, 12134.
[21] a) S. M. Sze, *Semiconductor Devices, Physics and Technology*, Wiley, New York **2002**. b) G. Horowitz, P. Lang, M. Mottaghi, H. Aubin, *Adv. Funct. Mater.* **2004**, *14*, 1069.
[22] J.-L. Brédas, D. Beljonne, V. Coropceanu, J. Cornil, *Chem. Rev.* **2004**, *104*, 4971.
[23] C. R. Newman, C. D. Frisbie, D. A. da Silva, J. L. Bredas, P. C. Ewbank, K. R. Mann, *Chem. Mater.* **2004**, *16*, 4436.
[24] D. A. da Silva, E. G. Kim, J.-L. Brédas, *Adv. Mater.* **2005**, *17*, 1072.
[25] V. Coropceanu, J. Cornil, D. A. daSilvaFilho, Y. Olivier, R. Silbey, J.-L. Brédas, *Chem. Rev.* **2007**, *107*, 926.
[26] Z. H. Li, M. S. Wong, Y. Tao, H. Fukutani, *Org. Lett.* **2007**, *9*, 3659.
[27] J. Ohshita, H. Kai, A. Takata, T. Iida, A. Kunai, N. Ohta, K. Komaguchi, M. Shiotani, A. Adachi, K. Sakamaki, K. Okita, *Organometallics* **2001**, *20*, 4800.
[28] R. Wu, J. S. Schumm, D. L. Pearson, J. M. Tour, *J. Org. Chem.* **1996**, *61*, 6906.
[29] C. Kloc, P. G. Simpkins, T. Siegrist, R. A. Laudise, *J. Cryst. Growth* **1997**, *182*, 416.
[30] C. Reese, Z. Bao, *Mater. Today* **2007**, *10*, 20.
[31] G. M. Sheldrick, *Acta Crystallogr. Sect. A* **2008**, *64*, 112.